

Reducing CO₂ to Methanol Using Frustrated Lewis Pairs: On the Mechanism of Phosphine–Borane-Mediated Hydroboration of CO₂

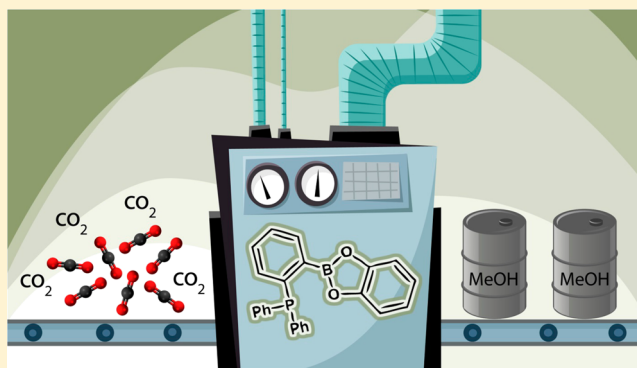
Marc-André Courtemanche,[†] Marc-André Légaré,[†] Laurent Maron,^{*,‡} and Frédéric-Georges Fontaine^{*,†}

[†]Département de Chimie, Centre de de Catalyse et Chimie Verte (C3V), Université Laval, 1045 Avenue de la Médecine, Québec, QC, Canada G1V 0A6

[‡]Université de Toulouse, INSA, UPS, LCPNO, CNRS, UMR 5215 CNRS-UPS-INSA, 135 avenue de Ranguel, Toulouse, France

S Supporting Information

ABSTRACT: The full mechanism of the hydroboration of CO₂ by the highly active ambiphilic organocatalyst 1-Bcat-2-PPh₂-C₆H₄ (Bcat = catecholboranyl) was determined using computational and experimental methods. The intramolecular Lewis pair was shown to be involved in every step of the stepwise reduction. In contrast to traditional frustrated Lewis pair systems, the lack of steric hindrance around the Lewis basic fragment allows activation of the reducing agent while moderate Lewis acidity/basicity at the active centers promotes catalysis by releasing the reduction products. Simultaneous activation of both the reducing agent and carbon dioxide is the key to efficient catalysis in every reduction step.



INTRODUCTION

The general concern over the increase in the CO₂ concentration in the atmosphere and its influence on climate change has led to several worldwide initiatives to control the emissions of this greenhouse gas. Although several carbon capture technologies have been developed, the possibility of using CO₂ as a C-1 feedstock to synthesize valuable chemicals could be an important financial incentive for reducing CO₂ emissions.¹ For these reasons, carbon dioxide transformation has attracted much scientific attention over the past decade.² Of particular interest and at the core of the methanol economy is the transformation of CO₂ into high-hydrogen-content hydrocarbons since such technology could help generate “green” energy vectors that are needed on a global scale to replace fossil fuels.³ Although most of the reported systems use heterogeneous catalysts, some homogeneous transition-metal-based catalytic systems have been developed for the reduction of CO₂ to formic acid,⁴ formate,⁵ formaldehyde,⁶ methanol,⁷ methane,⁸ and acetals.⁹

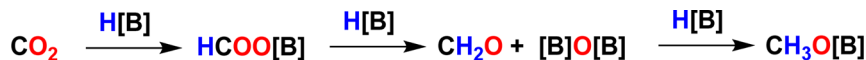
Organocatalysts, as species not composed of transition metals, are still scarce in the field of CO₂ functionalization to give valuable chemicals. Notable systems include highly Lewis acidic aluminum species¹⁰ and silyl cations,¹¹ which have been shown to reduce CO₂ with low selectivity to mixtures of products comprising methane, methanol, and a number of alkylation byproducts. Pioneering work by Stephan and Erker demonstrated the capacity of frustrated Lewis pairs (FLPs) to bind carbon dioxide, which led to the subsequent discovery of a number of ambiphilic systems capable of stoichiometric fixation.¹² However, except for the reduction of CO₂ to CO by carbodiphosphoranes,¹³ no other catalytic reduction of CO₂ has been reported for these systems. The PMes₃/AlX₃ (X = Cl, Br,

C₆F₅) FLP mediated the stoichiometric reduction of CO₂ using NH₃·BH₃, but the system had to be destroyed by hydrolysis in order to free the reduced methoxide fragment and generate methanol.¹⁴ Piers also developed an FLP-based catalytic reduction of CO₂ to methane by using hydrosilanes, albeit with limited turnovers.¹⁵ Ying and co-workers reported that N-heterocyclic carbenes can be used as catalysts to reduce CO₂ to methanol in the presence of hydrosilanes with a turnover frequency (TOF) of 25 h⁻¹ at room temperature.¹⁶ Recently, Cantat demonstrated that some nitrogen bases, such as guanidines and amidines, can be used as catalysts for the reduction of CO₂ to formamide using hydrosilanes¹⁷ or to methoxyboranes using 9-borabicyclo[3.3.1]nonane (9-BBN) and catecholborane (HBcat).¹⁸ Stephan also reported that phosphines can catalyze the reduction of CO₂ to methoxyboranes using 9-BBN as the reducing agent.¹⁹

Our group recently reported that the organocatalyst 1-Bcat-2-PPh₂-C₆H₄ (**1**), which can also be generated by the addition of HBcat to the precatalyst Al(2-PPh₂-C₆H₄)₃,²⁰ is highly active for the hydroboration of CO₂ to methoxyboranes, species that can be readily hydrolyzed to methanol, using a variety of hydroboranes.²¹ With catecholborane or high-hydrogen-content BH₃·SMe₂, a TOF of 973 h⁻¹ and turnover numbers (TONs) over 2950 were observed at a temperature of 70 °C. In a recent contribution, Wang and Stephan²² reported a similar ambiphilic system to be catalytically active in the hydroboration of CO₂. Both of these systems have in common the weak Lewis acidity of the borane compared with the strong Lewis acids normally used

Received: May 13, 2014

Published: June 20, 2014

Scheme 1. Schematic Representation of the Stepwise Hydroboration of CO₂ to Methoxyboranes Using Hydroboranes (H[B])

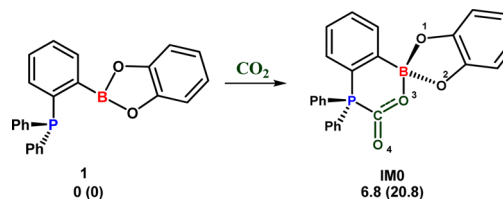
in classical FLP systems. Understanding the fundamental process of this catalytic system and identifying the important reaction intermediates is therefore of prime importance in order to unveil the full potential of ambiphilic molecules and FLPs as efficient catalysts. In order to determine the true role of the catalyst in every step of the reduction process, a thorough computational study has been carried out and complemented by experimental studies. Herein we report the full mechanism for the first metal-free catalytic hydroboration of CO₂ to methoxyboranes. A closer look at the critical steps of the reaction underlines some of the key aspects of the mechanism and offers an unprecedented insight and a novel way to approach ambiphilic molecule and FLP-mediated catalysis.

COMPUTATIONAL DETAILS

All of the calculations were performed on the full structures of the reported compounds. Calculations were performed with the Gaussian 03 and Gaussian 09 program suites.^{23,24} While the wB97XD functional²⁵ was qualified as promising by Grimme²⁶ and was used to accurately describe the mechanism of FLP-mediated hydrogenation of alkynes,²⁷ its use for modeling of **1** showed a very different geometry than the reported crystal structure.²¹ On the basis of the accurate description of **1** with respect to the reported structure, the B3PW91²⁸ functional was used in combination with the 6-31G** basis set for B, C, H, and O atoms²⁹ and the SDD basis set with an additional polarization function (one d function with an exponent of 0.34 and a contraction coefficient of 1.0) for the P atom.³⁰ The transition states were located and confirmed by frequency calculations (single imaginary frequency). Intrinsic reaction coordinate (IRC) calculations were performed to confirm the link between each transition state and the corresponding reactants and products. The stationary points were characterized as minima by full vibration frequency calculations (no imaginary frequency). All of the geometry optimizations were carried out without any symmetry constraints. The energies were then refined by single-point calculations to include dispersion at the B97D/6-31G** level of theory.³¹ The energies were further refined by single-point calculations to account for solvent effects using the SMD solvation model³² with benzene, the experimental solvent. The differences between the energies with and without the solvation model can be found in the Supporting Information. Since the entropic contribution in solution cannot be accurately predicted by standard quantum-mechanical calculations and is often greatly overestimated,³³ it was shown that enthalpy values are a better approximation. Thus, the energies are reported in terms of enthalpies with the free energies reported as italicized numbers in parentheses. Bond rotations and their associated transition states were not calculated as it is clear that their energies are much lower than the energy barriers associated with the reduction steps in such a system and are therefore trivial. All of the structures with their associated enthalpies and Gibbs free energies as well as their Cartesian coordinates are fully detailed in the Supporting Information.

RESULTS

At this point, it is very important to mention that the entropic contributions for gas-phase calculations have been shown to be overestimated by 50–60% for a two-component reaction.³⁴ Thus, for the majority of the reported reactions (where three components come together), the entropic contribution, and therefore the free energy, is expected to be greatly overestimated. Some strategies have been used to better estimate the entropic contribution, notably by performing the vibrational analysis at up to 1324 atm³⁵ to account for better entropy correction, but for

Scheme 2. Reaction of **1** with CO₂ To Generate **IM0**, Illustrating the Potential Binding Sites for HBcat

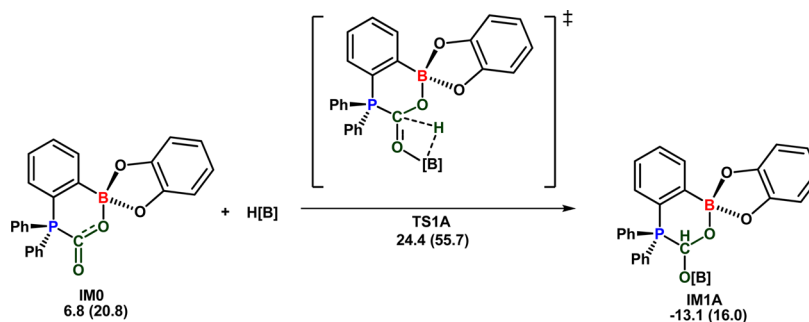
this study the free energies are provided without any correction. Even though entropic contributions are important and cannot be neglected, the enthalpy values provide more accurate comparisons for similar intermediates.

The hydroboration of carbon dioxide to methoxyboranes is a stepwise process that occurs through three subsequent reduction processes. First, CO₂ is reduced to a formatoborate, which is then reduced to formaldehyde. Finally, the formaldehyde is reduced to the methoxyborane (Scheme 1). The upcoming sections will consider these three reductions steps one by one in order to simplify the discussion.

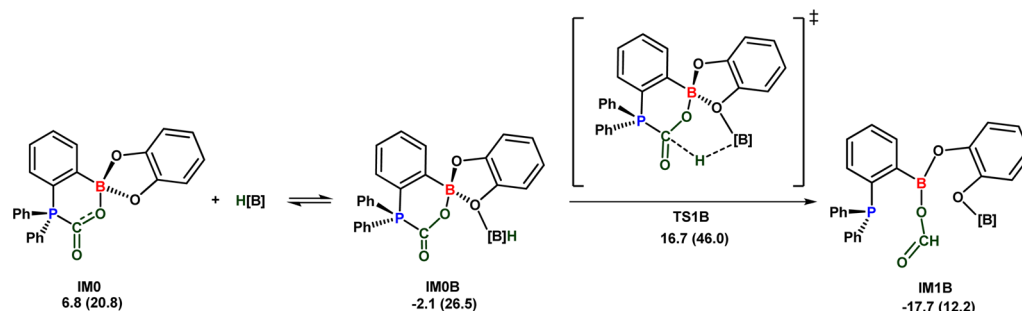
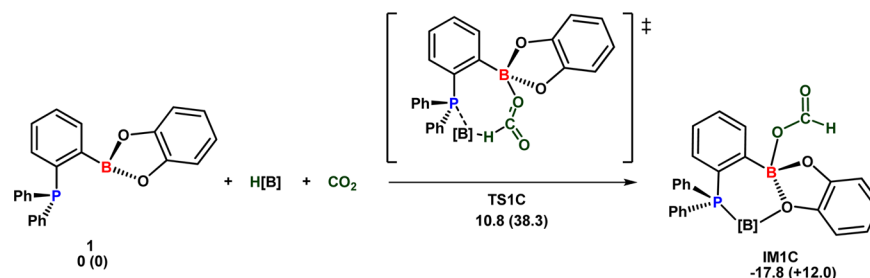
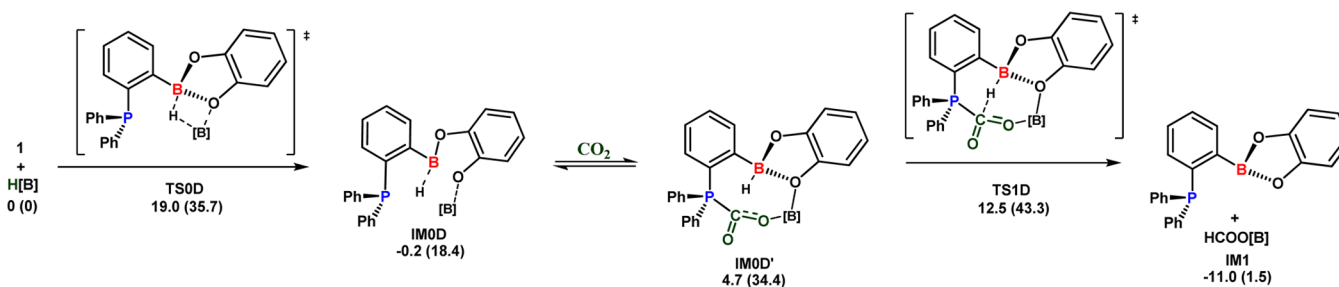
First Reduction Step: CO₂ to HCOOBcat. As expected, the direct reduction of carbon dioxide by HBcat is kinetically forbidden, as the associated transition state **TS1** was located +34.2 (+47.7) kcal·mol⁻¹ higher than the reactants. Experimental results support this hypothesis, as heating HBcat in the presence of 1 atm CO₂ at 70 °C for 48 h did not yield any observable CO₂ reduction product, even in the presence of PPh₃.²¹ Thus, a catalyst is required to lower the energy barrier and provide access to HCOOBcat (**IM1**, -11.0 (+1.5) kcal·mol⁻¹).

As was previously reported, the adduct between CO₂ and ambiphilic compound **1** (1-Bcat-2-PPh₂-C₆H₄) was never observed spectroscopically.²¹ Theoretical results suggest that the adduct formation between **1** and CO₂ is endothermic by +6.8 kcal·mol⁻¹ (**IM0**, +6.8 (+20.8) kcal·mol⁻¹). The binding of CO₂ induces a pyramidalization at the boron center, modifying the coordination environment of the catalyst. In fact, while the sum of the angles around the boron center in **1** is 359.9°, indicative of a planar sp² geometry, the sum of the same angles in **IM0** is 334.4°. Intermediate **IM0** counts four Lewis basic sites that can potentially bind HBcat. Indeed, coordination of the hydroborane to a nucleophilic site is required to promote the hydroboration of carbonyl-containing fragments.³⁶ In order to simplify the discussion, the Lewis basic sites are numbered 1 through 4, as illustrated in Scheme 2.

First, no transition state (TS) could be located for the reduction of CO₂ via the coordination of HBcat to site 1 or 3, mainly because of the geometric constraints that prevent the hydride transfer to the carbonyl moiety. Consequently, all four possible pathways for the initial reduction step (labeled A through D), involving coordination to the two remaining sites as well as direct coordination to the phosphorus atom of **1**, were studied and are described below. The most direct reduction path, pathway A (Scheme 3), involves the coordination of HBcat to site 4, generating the classical four-membered-ring hydroboration transition state (**TS1A**) as suggested by DiMare for the reduction of a variety of aldehydes and ketones by hydroboration.³⁶ For such a process, the barrier was found to

Scheme 3. Pathway A: Hydroboration Reaction of CO₂ through a Classical Four-Membered-Ring Transition State ([B] = Bcat)

Scheme 4. Pathway B: Hydroboration through Coordination of HBcat to the Catechol Fragment Followed by Intramolecular Hydride Delivery ([B] = Bcat)

Scheme 5. Pathway C: Hydroboration through Simultaneous Lewis Base Activation of the Borane and Lewis Acid Activation of CO₂ ([B] = Bcat)Scheme 6. Pathway D: CO₂ Reduction through the Generation of a Boronium/Hydridoborate Ion Pair ([B] = Bcat)

be relatively high but accessible at +24.4 (+55.7) kcal·mol⁻¹, generating IM1A (-13.1 (+16.0) kcal·mol⁻¹).³⁷ Therefore, pathway A does not appropriately represent the reduction of CO₂ to HCOOBcat by catalyst 1.

Coordination of HBcat to site 2 generates intermediate IM0B (-2.1 (+26.5) kcal·mol⁻¹), which is only slightly thermodynamically stabilized with respect to IM0 (pathway B; Scheme 4). From the adduct IM0B, the hydride can be transferred to the carbon atom of CO₂ through a six-membered-ring transition state (TS1B, +16.7 (+46.0) kcal·mol⁻¹), yielding IM1B (-17.7

(+12.2) kcal·mol⁻¹). Such reactivity is reminiscent of the hydroboration mechanism observed with oxazaborolidine catalysts developed by Corey and co-workers, where the coordination of the borane to a Lewis base promotes intramolecular hydride delivery.³⁸ It should be noted that pathway B is kinetically more accessible than pathway A since the TS is 7.7 kcal·mol⁻¹ lower in energy.

A third pathway can be considered in which the reducing agent and CO₂ are simultaneously activated. The phosphorus atom activates catecholborane, while CO₂ is activated by the boron

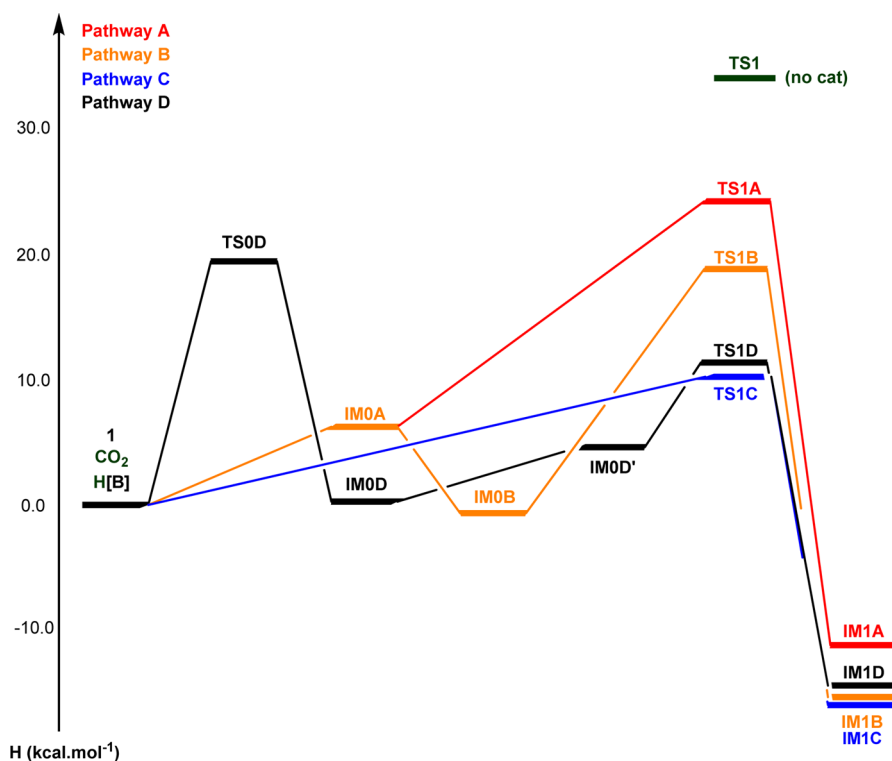
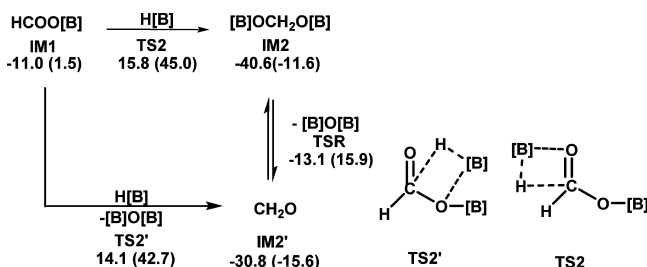
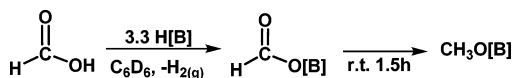


Figure 1. Relative enthalpies of important intermediates and transition states for the catalyzed reduction of CO₂ to HCOOBcat.

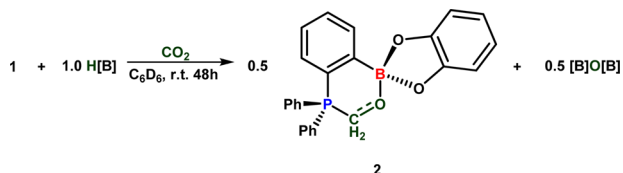
Scheme 7. Catalyst-Free Reduction of HCOOBcat to catBOCH₂OBcat or Formaldehyde [B]=Bcat



Scheme 8. Experimental Verification of the Hydroboration of Formic Acid by Catecholborane ([B] = Bcat)



Scheme 9. Attempt To Isolate HCOOBcat, Leading to the Exclusive Formation of 2 (IM2C'). [B]=Bcat

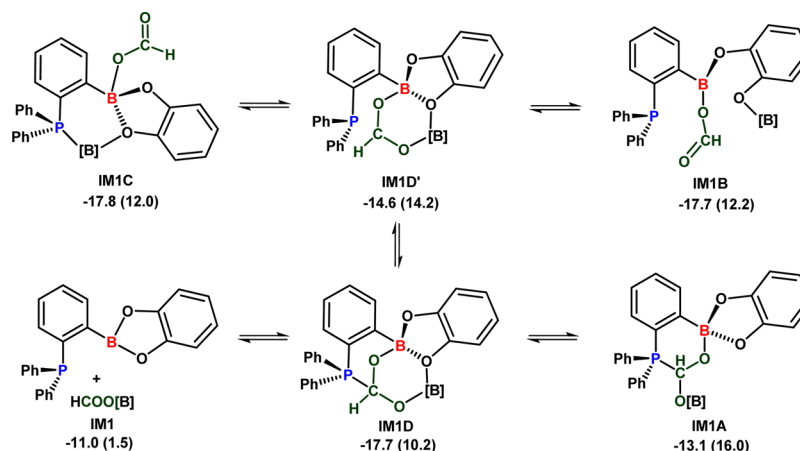


fragment. The coordination of the Lewis base increases the electronic density at the boron center, therefore making the hydride more nucleophilic. In fact, hydride activation of catecholborane by a variety of phosphines, including triphenylphosphine, has been reported in the past and was shown to occur readily at room temperature.³⁹ Hence, pathway C (Scheme 5)

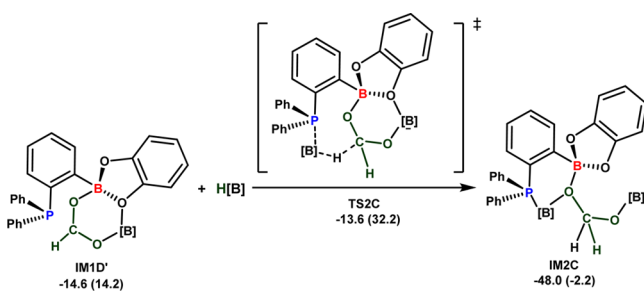
involving TS1C (+10.8 (+38.3) kcal·mol⁻¹) and leading to IM1C (-17.8 (+12.0) kcal·mol⁻¹) is even more energetically favorable than pathways A and B. The simultaneous activation of the reducing agent and the substrate drastically contrasts with the classical view of CO₂ activation by FLP systems, where the emphasis is on the sole activation of carbon dioxide by both functionalities. Very bulky groups on the catalyst framework, notably on the Lewis base, may restrict the interaction with the hydride source, decreasing the reactivity of the system.

Consistent with the experimental results, where no reaction was observed when catecholborane was heated in the presence of 1,²¹ no minimum was found on the potential energy surface for the formation of an adduct between HBcat and the catalyst. However, further theoretical investigation shows possible rearrangements leading to other plausible intermediates. Indeed, as represented in Scheme 6, HBcat can add to one of the B–O bonds of the catalyst through TS0D (+19.0 (+35.7) kcal·mol⁻¹) to generate intermediate IM0D (-0.2 (+18.4) kcal·mol⁻¹), which upon addition of CO₂ generates intermediate IM0D' (+4.7 (+34.4) kcal·mol⁻¹). The latter can be described as a hydridoborate/boronium bifunctional system in which the binding of CO₂ is ensured by the assistance of the catecholboronium fragment, which makes CO₂ more prone to nucleophilic attack. At the same time, the phosphine moiety acts as an anchor point, allowing the fixation of CO₂ with an ideal orientation for hydride delivery from the hydridoborate fragment. The hydride delivery occurs at TS1D (+12.5 (+43.3) kcal·mol⁻¹), leading to the regeneration of the catalyst by release of HCOOBcat. This completes an alternate reaction path for the initial step of CO₂ reduction (pathway D; Scheme 6). Such reactivity is somewhat reminiscent of the catalytic reduction of imines by boronium hydridoborate ion pairs as reported by Crudden and co-workers.⁴⁰

Scheme 10. Possible Interactions and Rearrangements of HCOOBcat with Catalyst 1 ([B] = Bcat)



Scheme 11. Suggested Pathway for the Catalyzed Reduction of HCOO[B] Involving the Catalyst ([B] = Bcat)



Summing up the results for the reduction of CO₂ to HCOOBcat (Figure 1), the direct hydroboration through pathway A can be ruled out. Although the activation of HBcat by one of the oxygen atoms of **1** (pathway B) or through hydride transfer from HBcat to the catalyst (pathway D) are plausible, pathway C is the most easily accessible and yields **IM1C** with a net energetic gain of 17.8 kcal·mol⁻¹. The catalyzed reduction leads to a decrease in the activation energy by 23.4 kcal·mol⁻¹ compared with the uncatalyzed system, making the reduction kinetically manageable.

Second Reduction Step: From HCOOBcat to CH₂O and Derivatives. Before the possible role of the catalyst in the second reduction step was determined, the uncatalyzed hydroboration of HCOOBcat was investigated thoroughly. From HCOOBcat (**IM1**), the reduction occurs through the classical four-membered-ring transition state **TS2** (+15.8 (+45.0) kcal·mol⁻¹) or **TS2'** (+14.1 (+42.7) kcal·mol⁻¹) to yield catBOCH₂OBcat (**IM2**, -40.6 (-11.6) kcal·mol⁻¹) or formaldehyde (**IM2'**, -30.8 (-15.6) kcal·mol⁻¹), respectively (Scheme 7; also see the Supporting Information). The transition state **TS2** was previously reported in the work of Wang and co-workers, but the authors concluded that the energy barrier was too high for the reactions to occur at room temperature.^{41a} On the other hand, it has been reported that the reaction of catecholborane with carboxylic acids of the type RCOOH (R = alkyl) at room temperature yields the corresponding acyloxboranes (RCOOBcat) as intermediates as well as H₂.⁴² The addition of two supplementary equivalents of HBcat results in the formation of RCH₂OBcat, leading to the corresponding alcohol after aqueous workup. In order to verify that the reduction of HCOOBcat by HBcat was indeed possible, the

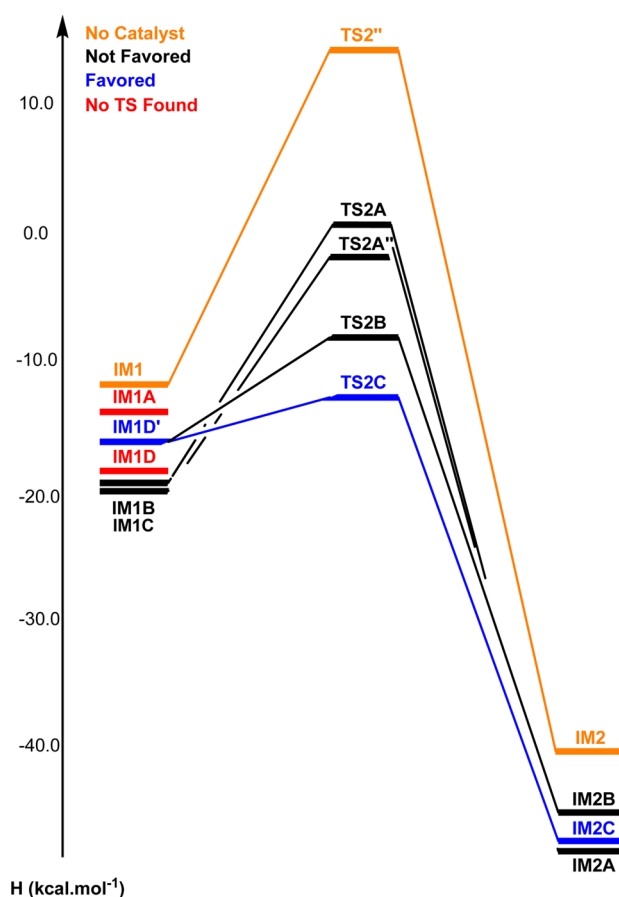


Figure 2. Relative enthalpies of transition states and intermediates for the reduction of HCOOBcat to CH₂O or catBOCH₂OBcat.

reaction between HBcat and formic acid (HCOOH) was studied experimentally.

The addition of formic acid (1 equiv) to a slight excess of catecholborane (3.3 equiv) at room temperature led to the rapid evolution of dihydrogen. As expected, monitoring of the reaction using ¹H NMR spectroscopy revealed the presence of HCOOBcat as an intermediate species, but after 90 min, the signals attributed to HCOOH and HBcat disappeared completely, resulting in total conversion to CH₃OBcat and catBOBcat (Scheme 8). The nature of the products was confirmed by ¹¹B{¹H} NMR spectroscopy and confirmed on

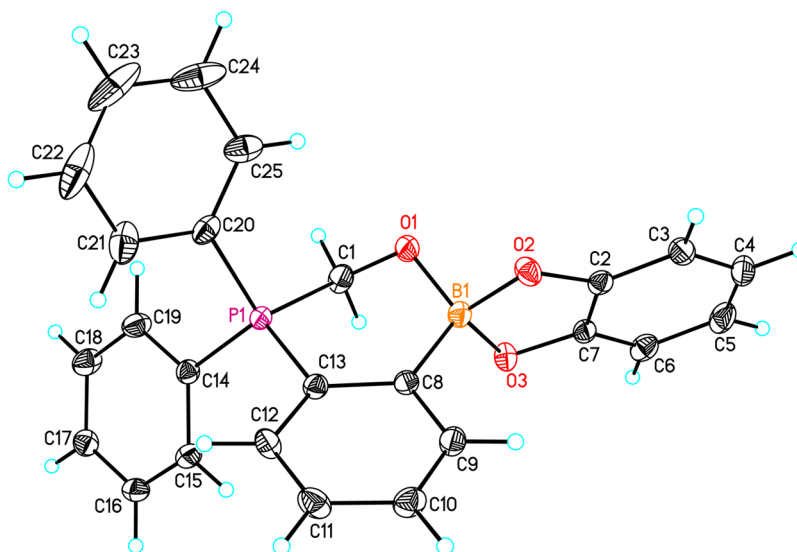
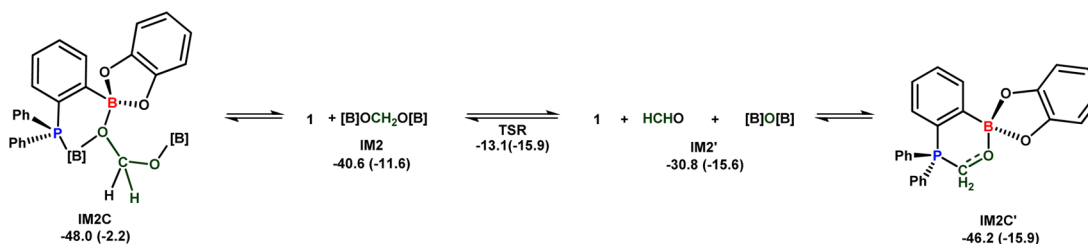
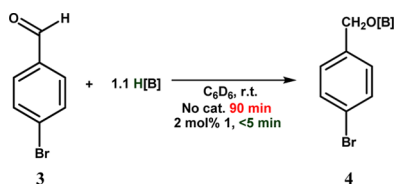


Figure 3. ORTEP drawing of **2** with the anisotropic atomic displacement ellipsoids shown at the 50% probability level. Selected bond lengths (Å) and angles (deg): P1–C1 1.823(2), C1–O1 1.402(3), O1–B1 1.473(3), C13–P1–C1 104.74(9), C8–C13–P1 117.28(14), C13–C8–B1 125.32(16), C1–O1–B1 113.67(15).

Scheme 12. Formation of IM2C' (**2**) through the Rearrangement of catBOCH₂OBcat to CH₂O ([B] = Bcat)



Scheme 13. Experimental Verification of the Catalytic Role of **1** in the Hydroboration of 4-Bromobenzaldehyde by Catecholborane ([B] = Bcat)



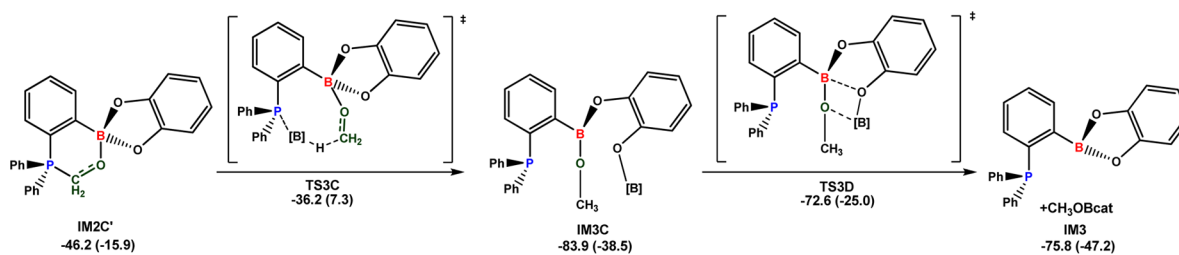
the basis of literature precedents.²⁰ Repeating the same experiment at 70 °C yielded complete conversion after only 15 min. With a computed barrier of +25.1 (+41.2) kcal·mol⁻¹ for the hydroboration of HCOOBcat by HBcat, it is clear that the reaction occurs much faster than previously assumed on the basis

of computational results and that HCOOBcat can be reduced without the implication of a catalyst.

However, in contrast to the other reported systems for the catalytic hydroboration of carbon dioxide where formatoborate species were observed during catalysis,^{6,7a,18} no trace of HCOOBcat was observed during catalysis with **1**.²¹ Indeed, no HCOOBcat could be detected even when the reaction with **1** equiv of HBcat relative to catalyst **1** under 1 atm CO₂ was monitored at room temperature. The only new species that was observed in this reaction mixture was the formaldehyde adduct **2** (Scheme 9). This result suggests that catalyst **1** plays an important role in the reduction of the formatoborate species. Such a result is in line with the previously reported results showing that **1** catalyzes the hydroboration of methyl formate.²¹

In order to reveal how this reduction step is catalyzed, the interaction of HCOOBcat (IM1) with catalyst **1** was studied computationally. The fact that the most favored interaction

Scheme 14. Catalyzed Reduction of Formaldehyde to CH₃OBcat with Regeneration of the Catalyst ([B] = Bcat)



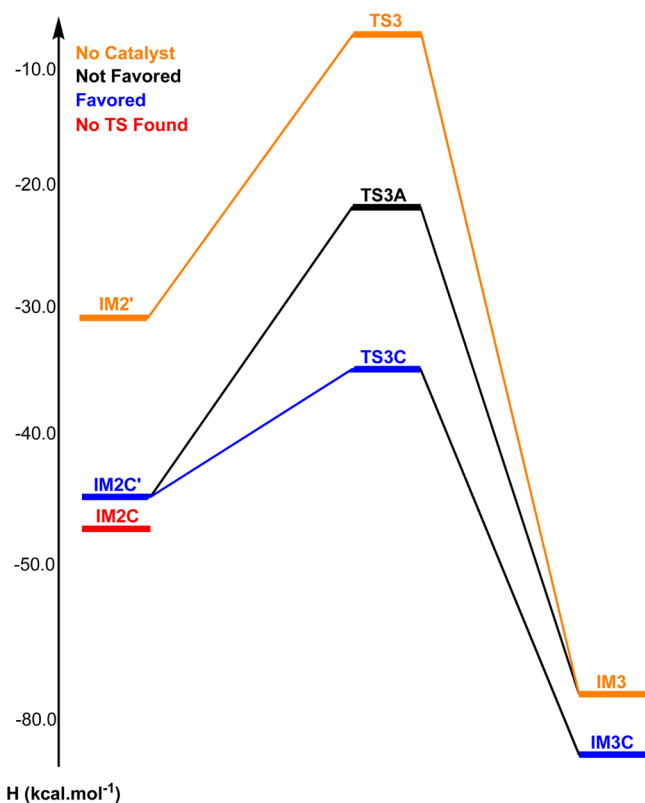


Figure 4. Relative enthalpies of transition states and intermediates for the reduction of CH_2O to CH_3OBcat .

(**IM1C**, -17.8 ($+12.0$) $\text{kcal}\cdot\text{mol}^{-1}$) was slightly exothermic by -6.8 $\text{kcal}\cdot\text{mol}^{-1}$ with respect to the free reagents suggests that some of the HCOOBcat molecules remain bound to the catalyst. However, each isomer observed in Scheme 10 can still be considered as a potential intermediate for the subsequent hydroboration reaction, and therefore, one must also take into account the possible rearrangements of **IM1C**.

Interestingly, no suitable transition state was found directly from **IM1D**. This is in line with the study by Musgrave and co-workers,⁴³ who demonstrated that even if the binding of a phosphine center to CO_2 is beneficial for the fixation of the CO_2 molecule on a catalyst, a strong $\text{P}-\text{C}$ interaction may actually hinder hydride transfer since the electrophilic site on carbon is occupied by the free electron pair of phosphorus. An interesting situation occurs in the case of **IM1D'**, in which the phosphine does not interact with the electrophilic carbon atom of the activated substrate. The activation of a HBcat molecule by the phosphorus moiety, as previously observed for pathway C, leads to hydride transfer through the most accessible TS for the reduction of HCOOBcat , **TS2C** (-13.6 ($+32.2$) $\text{kcal}\cdot\text{mol}^{-1}$), generating **IM2C** (-48.0 (-2.2) $\text{kcal}\cdot\text{mol}^{-1}$) with a net energetic gain of 34.4 $\text{kcal}\cdot\text{mol}^{-1}$ (Scheme 11).

Other pathways are also less favored, as the hydroborations through four-membered-ring transition states similar to pathway A, either from **IM1B** or **IM1C** and leading to $\text{catBOCH}_2\text{OBcat}$ -type reduction products, were found to be unlikely (see the Supporting Information). Alternately, hydride transfer through coordination of HBcat to the catechol oxygen atom of **IM1D**, similar to what was observed in pathway B (Scheme 4) and leading to formaldehyde and catBOBcat , although accessible, proved to be less favored than **TS2C** (see the Supporting Information). These results underline the beneficial effect of

double Lewis acid activation while reinforcing the concept of hydride activation by the Lewis basic center, since the catalyzed reduction is 20.9 $\text{kcal}\cdot\text{mol}^{-1}$ more favored than the catalyst-free reduction (Figure 2).

Third Reduction Step: Reducing CH_2O and Derivatives to CH_3OBcat . Although species **2** was previously characterized in solution, it was possible to observe in the reduction process at 25 $^\circ\text{C}$ the formation of a crystalline solid that was identified as the formaldehyde adduct, thus confirming the presence of this intermediate (Figure 3). The various bond lengths in the crystal structure of **2** are in accordance with the computational data, thus once more confirming the validity of the method.

Therefore, **IM2C** must rearrange to this more stable intermediate. Upon a closer look at **IM2C**, it is better described as a simple adduct between **1** and $\text{catBOCH}_2\text{OBcat}$ in which the interactions occur through dative $\text{P}-\text{B}$ and $\text{B}-\text{O}$ bonds. However, the binding is favored by only -7.4 ($+9.4$) $\text{kcal}\cdot\text{mol}^{-1}$. As can be observed in Scheme 12, $\text{catBOCH}_2\text{OBcat}$ may rearrange to generate CH_2O by releasing catBOBcat (**IM2'**, -30.8 (-15.6) $\text{kcal}\cdot\text{mol}^{-1}$). Such a rearrangement was also assumed to happen by Wang et al.⁴¹ in their related theoretical study of a catalytic CO_2 hydroboration system. The system is then stabilized by the trapping of formaldehyde by **1** to generate **IM2C'** (**2**). The entropic stabilization due to the release of a catBOBcat molecule is thought to be the driving force for the formation of this intermediate.

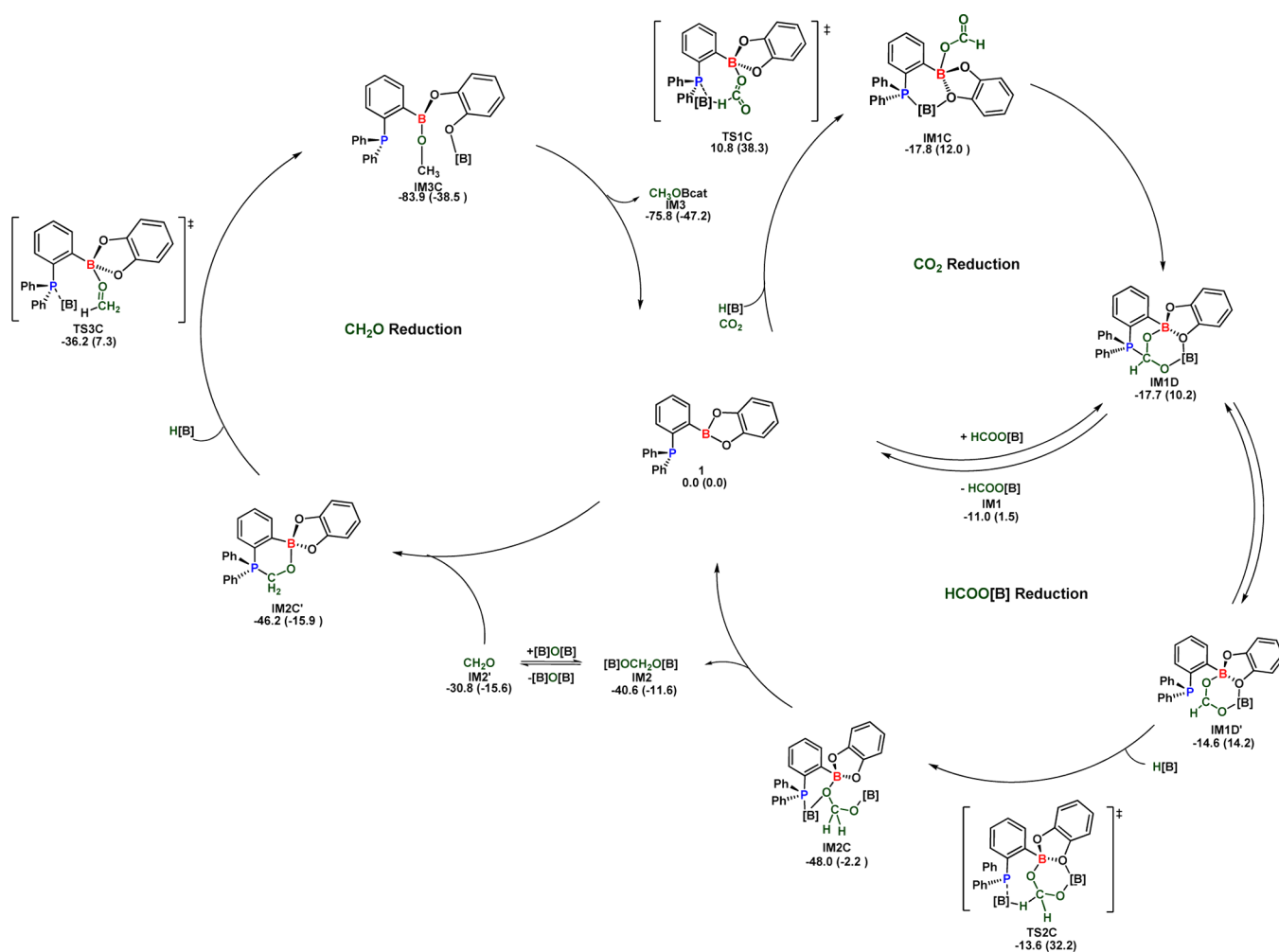
It is widely known that aldehydes are readily reduced by hydroboranes, but we were curious to see whether the trapping of formaldehyde by catalyst **1** would hinder or favor the reduction. Since formaldehyde readily polymerizes to paraformaldehyde and the solubility of **2** in common NMR solvents is very limited, 4-bromobenzaldehyde (**3**) was chosen as a model compound. Monitoring of the reaction between **3** and 1.1 equiv of HBcat showed that the reduction takes 90 min to yield complete conversion to the corresponding alkoxyborane **4**. Interestingly, repeating the reaction under identical conditions but in the presence of 2 mol % **1** led to the complete conversion in less than 5 min (Scheme 13), showing that **1** acts as a catalyst for the reduction of aldehydes to alkoxyboranes.

This interesting result prompted us to investigate this final step computationally. From the formaldehyde adduct **IM2C'** (**2**), activation of HBcat by the phosphine moiety (similar to pathway C) leads to **TS3C** (-36.2 ($+7.3$) $\text{kcal}\cdot\text{mol}^{-1}$), yielding the intermediate **IM3C** (-83.9 (-38.5) $\text{kcal}\cdot\text{mol}^{-1}$). It should be noted that **IM3C** can easily rearrange to **IM3** through **TS3D** (-72.6 (-25.0) $\text{kcal}\cdot\text{mol}^{-1}$), regenerating catalyst **1** and producing CH_3OBcat (Scheme 14).

The final reduction step represents an energetic gain of 25.8 $\text{kcal}\cdot\text{mol}^{-1}$. The catalyzed reduction is 10.2 $\text{kcal}\cdot\text{mol}^{-1}$ more favored than the catalyst-free reduction (Figure 4). All other pathways (similar to pathways A and B) are less favorable (see the Supporting Information).

DISCUSSION

As discussed above, the catalyst is essential to lower the energy gap in order to allow the reduction of CO_2 to HCOOBcat to occur, but it also plays a significant role in enhancing the rates of the subsequent reduction steps. The most favorable species for the reduction in the first step is one in which the Lewis acidic site of the catalyst binds CO_2 while the phosphine activates the borane to deliver a hydride to the activated electrophilic carbon of carbon dioxide. Together, these factors lead to a lowering of the energy barrier by 23.4 $\text{kcal}\cdot\text{mol}^{-1}$ compared with the catalyst-

Scheme 15. Proposed Mechanistic Pathway (Including Important Transition States) for the Reduction of CO₂ to CH₃OBcat by 1 ([B] = Bcat)

free reduction. This pathway puts emphasis on the fact that the role of the catalyst is to simultaneously activate both of the reagents and not CO₂ alone.

The reductions of both HCOOBcat and CH₂O were shown to be possible without any implication from the catalyst, and consequently, some of these reductions are expected to occur catalyst-free in the presence of a large excess of HBcat. However, activation of the HBcat moiety by the phosphorus center while the substrate is fixed and activated by the Lewis acidic boron center results in lowering of the transition state energies by 20.9 and 10.2 kcal·mol⁻¹ for the hydroboration of HCOOBcat and CH₂O respectively. The rapid reduction of HCOOBcat by the catalyst and in the reaction medium explains why it could not be observed experimentally. On the other hand, the 15.4 kcal·mol⁻¹ bonding interaction of the catalyst with formaldehyde rationalizes the fact that this particular adduct can be observed by NMR spectroscopy during catalysis. As was found out in this study, **2** even crystallizes out of the reaction medium at ambient temperature, while everything is soluble at 70 °C. This aspect might explain the lower activity of this system at room temperature and the high enhancement of the catalytic turnovers with a relatively slight increase in temperature. The entire catalytic process is summarized in Scheme 15.

When these results are taken into account, the classical FLP approach of using very bulky substituents may lead to more

difficult activation of substrates. While a strongly Lewis basic phosphine might bind CO₂ and other intermediates more strongly and hinder hydride transfer, it may also activate the reductant more effectively and increase the catalytic activity. However, the use of a moderate Lewis acid allows the release of the various hydroboration products in the reaction medium, allowing their liberation from the catalyst. A key aspect of the system is the presence of both the Lewis acid and base in a single molecule, reducing the entropic cost of every catalyzed step. Finally, the importance of the oxygen substituents on the boron center cannot be overlooked, as their dynamic nature allows the formation of a number of isomers and intermediates for a very flexible catalyst.

CONCLUSION

The full mechanism for the first catalytic hydroboration of carbon dioxide by an FLP-based system, **1**, was determined. The catalyst was shown to catalyze every step of the reaction. The findings reported herein offer important insight into the aspects that need to be considered for the design of ambiphilic catalysts. Current work is focused on preparing new ambiphilic catalysts by varying the functional groups on phosphorus and boron in order to achieve maximal catalytic efficiency and broaden the scope of reducing agents to hydrosilanes. We are hopeful that these

findings will inspire unprecedented FLP chemistry and novel catalytic applications.

■ ASSOCIATED CONTENT

■ Supporting Information

Detailed experimental procedures and additional DFT information, including other calculated reaction pathways, Cartesian coordinates, and enthalpies and free energies. This material is available free of charge via the Internet at <http://pubs.acs.org>.

■ AUTHOR INFORMATION

Corresponding Authors

frederic.fontaine@chm.ulaval.ca
laurent.maron@irsamc.ups-tlse.fr

Notes

The authors declare no competing financial interest.

■ ACKNOWLEDGMENTS

This work was supported by the National Sciences and Engineering Research Council (NSERC) of Canada and the Centre de Catalyse et Chimie Verte (Quebec). M.-A.C. and M.-A.L. thank NSERC and FQRNT for scholarships. We acknowledge R. Nadeau for the TOC graphic, W. Bi for the resolution of the crystal structure, and D. Bourissou for insightful discussions. L.M. is member of the Institut Universitaire de France. Cines and CALMIP are acknowledged for a generous grant of computing time. The Humboldt Foundation is also acknowledged for financial support.

■ REFERENCES

- (1) Olah, G. A.; Goepfert, A.; Surya Prakash, G. K. *J. Org. Chem.* **2009**, *74*, 487–498.
- (2) D'Alessandro, D. M.; Smit, B.; Long, J. R. *Angew. Chem., Int. Ed.* **2010**, *49*, 6058–6082.
- (3) Olah, G. A.; Goepfert, A.; Surya Prakash, G. K. *Beyond Oil and Gas: The Methanol Economy*; Wiley-VCH: Weinheim, Germany, 2006.
- (4) (a) Tanaka, R.; Yamashita, M.; Nozaki, K. *J. Am. Chem. Soc.* **2009**, *131*, 14168–14169. (b) Federsel, C.; Jackstell, R.; Beller, M. *Angew. Chem., Int. Ed.* **2010**, *49*, 6254–6257. (c) Schaub, T.; Paciello, R. A. *Angew. Chem., Int. Ed.* **2011**, *50*, 7278–7282.
- (5) (a) Langer, R.; Diskin-Posner, Y.; Leitus, G. W.; Shimon, L. J.; Ben-David, Y.; Milstein, D. *Angew. Chem., Int. Ed.* **2011**, *50*, 9948–9952. (b) Federsel, C.; Boddien, A.; Jackstell, R.; Jennerjahn, R.; Dyson, P. J.; Scopelliti, R.; Laurenczy, G.; Beller, M. *Angew. Chem., Int. Ed.* **2010**, *49*, 9777–9780. (c) Huff, C. A.; Sanford, M. S. *ACS Catal.* **2013**, *3*, 2412–2416. (d) Jeletic, M. S.; Mock, M. T.; Appel, A. M.; Linehan, J. C. *J. Am. Chem. Soc.* **2013**, *135*, 11533–11536. (e) Zhang, L.; Cheng, J.; Hou, Z. *Chem. Commun.* **2013**, *49*, 4782–4784. (f) Shintani, R.; Nozaki, K. *Organometallics* **2013**, *32*, 2459–2462. (g) Suh, H.-J.; Guard, L. M.; Hizari, N. *Chem. Sci.* **2014**, DOI: 10.1039/C4SC01110D.
- (6) Bontemps, S.; Sabo-Etienne, S. *Angew. Chem., Int. Ed.* **2013**, *52*, 10253–10255. (b) Bontemps, S.; Vendier, L.; Sabo-Etienne, S. *J. Am. Chem. Soc.* **2014**, *136*, 4419–4425.
- (7) (a) Chakraborty, S.; Zhang, J.; Krause, J. A.; Guan, H. *J. Am. Chem. Soc.* **2010**, *132*, 8872–8873. (b) Balaraman, E.; Gunanathan, C.; Zhang, J.; Shimon, L. J. W.; Milstein, D. *Nat. Chem.* **2011**, *3*, 609–614. (c) Huff, C. A.; Sanford, M. S. *J. Am. Chem. Soc.* **2011**, *133*, 18122–18125. (d) Wesselbaum, S.; von Stein, T.; Klankermayer, J.; Leitner, W. *Angew. Chem., Int. Ed.* **2012**, *51*, 7499–7502.
- (8) (a) Matsuo, T.; Kawaguchi, H. *J. Am. Chem. Soc.* **2006**, *128*, 12362–12363. (b) Park, S.; Bézier, D.; Brookhart, M. *J. Am. Chem. Soc.* **2012**, *134*, 11404–11407. (c) Mitton, S. J.; Turculet, L. *Chem.—Eur. J.* **2012**, *48*, 15258–15262. (d) Berkefeld, A.; Piers, W. E.; Parvez, M.; Castro, L.; Maron, L.; Eisenstein, O. *Chem. Sci.* **2013**, *4*, 2152–2162.

- (9) LeBlanc, F. A.; Piers, W. E.; Parvez, M. *Angew. Chem., Int. Ed.* **2014**, *126*, 808–811.
- (10) (a) Khandelwal, M.; Wehmschulte, R. J. *Angew. Chem., Int. Ed.* **2012**, *51*, 7323–7326. (b) Wehmschulte, R. J.; Saleh, M.; Powell, D. R. *Organometallics* **2013**, *32*, 6812–6819.
- (11) Schäfer, A.; Saak, W.; Haase, D.; Müller, T. *Angew. Chem., Int. Ed.* **2012**, *51*, 2981–2984.
- (12) (a) Mömning, C.; Otten, M.; Kehr, E. G.; Fröhlich, R.; Grimme, S.; Stephan, D. W.; Erker, G. *Angew. Chem., Int. Ed.* **2009**, *48*, 6643–6646. (b) Appelt, C.; Westenberg, H.; Bertini, F.; Ehlers, A. W.; Slootweg, J. C.; Lammertsma, K.; Uhl, W. *Angew. Chem., Int. Ed.* **2011**, *50*, 3925–3928. (c) Boudreau, J.; Courtemanche, M.-A.; Fontaine, F.-G. *Chem. Commun.* **2011**, *47*, 11131–11133. (d) Peuser, I.; Neu, R. C.; Zhao, X.; Ulrich, M.; Schirmer, B.; Tannert, J. A.; Kehr, G.; Fröhlich, R.; Grimme, S.; Erker, G.; Stephan, D. W. *Chem.—Eur. J.* **2011**, *17*, 9640–9650. (e) Hounjet, L. J.; Caputo, C. B.; Stephan, D. W. *Angew. Chem., Int. Ed.* **2012**, *51*, 4714–4717. (f) Takeuchi, K.; Stephan, D. W. *Chem. Commun.* **2012**, *48*, 11304–11306. (g) Theuergarten, E.; Schlösser, J.; Schllins, D.; Freytag, M.; Daniliuc, C. G.; Jones, P. G.; Tamm, M. *Dalton Trans.* **2012**, *41*, 9101–9110. (h) Lu, Z.; Liu, Y. J.; Wang, Y.; Lin, J.; Li, Z. H.; Wang, H. *Organometallics* **2013**, *32*, 6753–6758. (i) Barry, B. M.; Dickie, D. A.; Murphy, L. J.; Clyburne, J. A. C.; Kemp, R. A. *Inorg. Chem.* **2013**, *52*, 8312–8314.
- (13) Dobrovetsky, R.; Stephan, D. W. *Angew. Chem., Int. Ed.* **2013**, *52*, 2516–2519.
- (14) (a) Ménard, G.; Stephan, D. W. *J. Am. Chem. Soc.* **2010**, *132*, 1796–1797. (b) Ménard, G.; Stephan, D. W. *J. Am. Chem. Soc.* **2010**, *132*, 1796–1797. (c) Ménard, G.; Stephan, D. W. *Dalton Trans.* **2013**, *42*, 5447–5453. (d) Roy, L.; Zimmerman, P. M.; Paul, A. *Chem.—Eur. J.* **2011**, *17*, 435–439. (e) Ménard, G.; Gilbert, T. M.; Hatnean, J. A.; Kraft, A.; Krossing, I.; Stephan, D. W. *Organometallics* **2013**, *32*, 4416–4422.
- (15) (a) Berkefeld, A.; Piers, W. E.; Parvez, M. *J. Am. Chem. Soc.* **2010**, *132*, 10660–10661. (b) Wen, M.; Huang, F.; Lu, G.; Wang, Z.-X. *Inorg. Chem.* **2013**, *52*, 12098–12107. (c) Ashley, A. E.; Thompson, A. L.; O'Hare, D. *Angew. Chem., Int. Ed.* **2009**, *48*, 9839–9843.
- (16) Riduan, S. N.; Zhang, Y.; Ying, J. Y. *Angew. Chem., Int. Ed.* **2009**, *48*, 3322–3325.
- (17) (a) Das Neves Gomes, C.; Jacquet, O.; Villiers, C.; Thuéry, P.; Ephritikhine, M.; Cantat, T. *Angew. Chem., Int. Ed.* **2012**, *51*, 187–190. (b) Jacquet, O.; Das Neves Gomes, C.; Ephritikhine, M.; Cantat, T. *J. Am. Chem. Soc.* **2012**, *134*, 2934–2937.
- (18) Das Neves Gomes, C.; Blondiaux, E.; Thuéry, P.; Cantat, T. *Chem.—Eur. J.* **2014**, *23*, 7098–7106.
- (19) Wang, T.; Stephan, D. W. *Chem. Commun.* **2014**, *50*, 7007–7010.
- (20) Courtemanche, M.-A.; Larouche, J.; Légaré, M.-A.; Wenhua, B.; Maron, L.; Fontaine, F.-G. *Organometallics* **2013**, *32*, 6804–6811.
- (21) (a) Courtemanche, M.-A.; Légaré, M.-A.; Maron, L.; Fontaine, F.-G. *J. Am. Chem. Soc.* **2013**, *135*, 9326–9329. (b) Fontaine, F.-G.; Courtemanche, M.-A.; Légaré, M.-A. *Chem.—Eur. J.* **2014**, *20*, 2990–2996.
- (22) Wang, T.; Stephan, D. W. *Chem.—Eur. J.* **2014**, *20*, 3036–3039.
- (23) Frisch, M. J.; Trucks, G. W.; Schlegel, H. B.; Scuseria, G. E.; Robb, M. A.; Montgomery, J. A., Jr.; Vreven, T.; Kudin, K. N.; Burant, J. C.; Millam, J. M.; Iyengar, S. S.; Tomasi, J.; Barone, V.; Mennucci, B.; Cossi, M.; Scalmani, G.; Rega, N.; Petersson, G. A.; Nakatsuji, H.; Hada, M.; Ehara, M.; Toyota, K.; Fukuda, R.; Hasegawa, J.; Ishida, M.; Nakajima, T.; Honda, Y.; Kitao, O.; Nakai, H.; Klene, M.; Li, X.; Knox, J. E.; Hratchian, H. P.; Cross, J. B.; Bakken, V.; Adamo, C.; Jaramillo, J.; Gomperts, R.; Stratmann, R. E.; Yazyev, O.; Austin, A. J.; Cammi, R.; Pomelli, C.; Ochterski, J. W.; Ayala, P. Y.; Morokuma, K.; Voth, G. A.; Salvador, P.; Dannenberg, J. J.; Zakrzewski, V. G.; Dapprich, S.; Daniels, A. D.; Strain, M. C.; Farkas, O.; Malick, D. K.; Rabuck, A. D.; Raghavachari, K.; Foresman, J. B.; Ortiz, J. V.; Cui, Q.; Baboul, A. G.; Clifford, S.; Cioslowski, J.; Stefanov, B. B.; Liu, A. L. G.; Piskorz, P.; Komaromi, I.; Martin, R. L.; Fox, D. J.; Keith, T.; Al-Laham, M. A.; Peng, C.; Nanayakkara, A.; Challacombe, M.; Gill, P. M. W.; Johnson, B.; Chen, W.; Wong, M.; Gonzalez, C.; Pople, J. A. *Gaussian 03*, revision D.01; Gaussian, Inc.: Wallingford, CT, 2004.

- (24) Frisch, M. J.; Trucks, G. W.; Schlegel, H. B.; Scuseria, G. E.; Robb, M. A.; Cheeseman, J. R.; Scalmani, G.; Barone, V.; Mennucci, B.; Petersson, G. A.; Nakatsuji, H.; Caricato, M.; Li, X.; Hratchian, H. P.; Izmaylov, A. F.; Bloino, J.; Zheng, G.; Sonnenberg, J. L.; Hada, M.; Ehara, M.; Toyota, K.; Fukuda, R.; Hasegawa, J.; Ishida, M.; Nakajima, T.; Honda, Y.; Kitao, O.; Nakai, H.; Vreven, T.; Montgomery, J. A., Jr.; Peralta, J. E.; Ogliaro, F.; Bearpark, M.; Heyd, J. J.; Brothers, E.; Kudin, K. N.; Staroverov, V. N.; Kobayashi, R.; Normand, J.; Raghavachari, K.; Rendell, A.; Burant, J. C.; Iyengar, S. S.; Tomasi, J.; Cossi, M.; Rega, N.; Millam, J. M.; Klene, M.; Knox, J. E.; Cross, J. B.; Bakken, V.; Adamo, C.; Jaramillo, J.; Gomperts, R.; Stratmann, R. E.; Yazyev, O.; Austin, A. J.; Cammi, R.; Pomelli, C.; Ochterski, J. W.; Martin, R. L.; Morokuma, K.; Zakrzewski, V. G.; Voth, G. A.; Salvador, P.; Dannenberg, J. J.; Dapprich, S.; Daniels, A. D.; Farkas, Ö.; Foresman, J. B.; Ortiz, J. V.; Cioslowski, J.; Fox, D. J. *Gaussian 09*, revision C.01; Gaussian, Inc.: Wallingford, CT, 2009.
- (25) Chai, J.-D.; Head-Gordon, M. *Phys. Chem. Chem. Phys.* **2008**, *10*, 6615–6620.
- (26) Grimme, S.; Goerigk, L. *Phys. Chem. Chem. Phys.* **2011**, *13*, 6670–6688.
- (27) Chernichenko, K.; Madarász, Á.; Pápai, I.; Nieger, M.; Leskelä, M.; Repo, T. *Nat. Chem.* **2013**, *5*, 718–723.
- (28) (a) Becke, A. D. *J. Chem. Phys.* **1993**, *98*, 5648–5652. (b) Burke, K.; Perdew, J. P.; Wang, Y. In *Electronic Density Functional Theory: Recent Progress and New Directions*; Dobson, J. F., Vignale, G., Das, M. P., Eds.; Springer: Berlin, 1998.
- (29) (a) Francl, M. M.; Pietro, W. J.; Hehre, W. J.; Binkley, J. S.; Gordon, M. S.; Defrees, D. J.; Pople, J. A. *J. Chem. Phys.* **1982**, *77*, 3654–3665. (b) Hehre, W. J.; Ditchfield, R.; Pople, J. A. *J. Chem. Phys.* **1972**, *56*, 2257–2261.
- (30) Andrae, D.; Heussermann, U.; Dolg, M.; Stoll, H.; Preuss, H. *Theor. Chim. Acta.* **1990**, *77*, 123–141.
- (31) Grimme, S. *J. Comput. Chem.* **2006**, *27*, 1787–1799.
- (32) Marenich, A. V.; Cramer, C. J.; Truhlar, D. G. *J. Phys. Chem. B* **2009**, *113*, 6378–6396.
- (33) (a) Huang, D.; Makhlynets, O. V.; Tan, L. L.; Lee, S. C.; Rybak-Akimova, E. V.; Holm, R. H. *Inorg. Chem.* **2011**, *50*, 10070–10081. (b) Huang, D. G.; Makhlynets, O. V.; Tan, L. L.; Lee, S. C.; Rybak-Akimova, E. V.; Holm, R. H. *Proc. Natl. Acad. Sci. U.S.A.* **2011**, *108*, 1222–1227. (c) Zhang, C. G.; Zhang, R.; Wang, Z. X.; Zhou, Z.; Zhang, S. B.; Chen, Z. *Chem.—Eur. J.* **2009**, *15*, 5910–5919. (d) Chen, Y.; Ye, S.; Jiao, L.; Liang, Y.; Sinha-Mahapatra, D. K.; Herndon, J. W.; Yu, Z. X. *J. Am. Chem. Soc.* **2007**, *129*, 10773–10784. (e) Yu, Z. X.; Houk, K. N. *J. Am. Chem. Soc.* **2003**, *125*, 13825–13830.
- (34) Liang, Y.; Liu, S.; Xia, Y. Z.; Li, Y. H.; Yu, Z. X. *Chem.—Eur. J.* **2008**, *14*, 4361–4373.
- (35) (a) Martin, R. L.; Hay, P. J.; Platt, L. R. *J. Phys. Chem. A* **1998**, *102*, 3565–3573. (b) Siffert, N.; Buehl, M. *J. Am. Chem. Soc.* **2010**, *132*, 8056–8070.
- (36) DiMare, M. *J. Org. Chem.* **1996**, *61*, 8378–8385.
- (37) All attempts to isolate an intermediate in which CO₂ was coordinated only to the phosphine moiety while being reduced by HBcat led to **TS1A**.
- (38) (a) Corey, E. J.; Link, J. O. *Tetrahedron Lett.* **1989**, *30*, 6275–6278. (b) Corey, E. J.; Bakshi, R. K. *Tetrahedron Lett.* **1990**, *31*, 611–614.
- (39) Westcott, S. A.; Blom, H. P.; Marder, T. B.; Baker, R. T.; Calabrese, J. C. *Inorg. Chem.* **1993**, *32*, 2175–2182.
- (40) Eisenberger, P.; Bailey, A. M.; Crudden, C. M. *J. Am. Chem. Soc.* **2012**, *134*, 17384–17387. Generation of the hydridoborate/boronium ion pair was also considered to occur through coordination to phosphine or from **IM0A**, but the TSs were found to be higher in energy (see the Supporting Information).
- (41) (a) Huang, F.; Zhang, C.; Jiang, J.; Wang, Z.-X.; Guan, H. *Inorg. Chem.* **2011**, *50*, 3816–3825. (b) Huang, F.; Lu, G.; Zhao, L.; Li, H.; Wang, Z.-X. *J. Am. Chem. Soc.* **2010**, *132*, 12388–12396.
- (42) Kabalka, G. W.; Baker, J. D.; Neal, G. W. *J. Org. Chem.* **1977**, *42*, 512–517.
- (43) Lim, C.-H.; Holder, A. M.; Hynes, J. T.; Musgrave, C. B. *Inorg. Chem.* **2013**, *52*, 10062–10066.